Appl Magn Reson
DOI 10.1007/s00723-011-0224-6

Applied
Magnetic Resonance

Fullerene C_{70} Triplet Zero-Field Splitting Parameters Revisited by Light-Induced EPR at Thermal Equilibrium

Mikhail N. Uvarov · Leonid V. Kulik · Sergei A. Dzuba

Received: 13 December 2010 / Revised: 23 March 2011

Abstract Continuous-wave (CW) electron paramagnetic resonance (EPR) and echo-detected (ED) EPR spectra of triplet state of fullerene C_{70} in molecular glasses of decalin, *o*-terphenyl and toluene, and in polymethylmethacrylate polymer were obtained under continuous light illumination. Temperature was high enough so that the EPR spectra corresponded to thermal equilibrium between the spin sublevels. The comparison of CW EPR and ED EPR data has shown that pseudorotation in the $^3C_{70}$ frame does not remarkably affect deriving the zero-field splitting (ZFS) *D* and *E* parameters from the EPR spectra. $^3C_{70}$ EPR spectra were simulated at 77 K fairly well using the distribution of the ZFS *D* and *E* parameters. These distributions may be caused by the inhomogeneity of the glassy matrix surrounding, which affects the Jahn–Teller distortions of $^3C_{70}$ molecules (*D*-strain and *E*-strain).

1 Introduction

Due to efficient light absorption, fullerenes and their derivatives are perspective for practical applications in solar energy engineering [1] and as a "free radical sponge" in medicine [2]. Under visible or ultraviolet (UV) light illumination, and in the absence of electron donors, fullerene C_{70} is converted to a lower triplet state, $^3C_{70}$, with quantum yield close to unity. The photophysical properties of fullerenes are described, e.g., in Ref. [3]. The $^3C_{70}$ state may be directly investigated by electron paramagnetic resonance (EPR).

M. N. Uvarov · L. V. Kulik (✉) · S. A. Dzuba
Institute of Chemical Kinetics and Combustion, Institutskaya 3, 630090 Novosibirsk, Russia
e-mail: chemphy@kinetics.nsc.ru

S. A. Dzuba
Novosibirsk State University, Pirogova 2, 630090 Novosibirsk, Russia

Published online: 21 April 2011

The $^3C_{70}$ zero-field splitting (ZFS) parameters D and E were obtained in several works, using different EPR techniques [4–13]. Their results are summarized in Table 1. Simulations of time-resolved EPR spectra of $^3C_{70}$ were performed [5–8] using dynamical models of the triplet molecule pseudorotation (dynamic Jahn–Teller effect). In other works [9–12], optically detected (OD) EPR resonance spectra of $^3C_{70}$ were obtained. In some cases, ZFS parameters were assumed to be distributed [11, 12]. Electron–nuclear double resonance (ENDOR) studies have shown that the sign of D value is positive [14].

In earlier works, the attempts were made to determine the $^3C_{70}$ ZFS parameters by semiempirical quantum chemical calculations [15]. It was understood that the situation is severely complicated by the Jahn–Teller effect in the $^3C_{70}$ frame, which decreases the initial D_{5d} symmetry of the C_{70} ground state. Despite numerous attempts, symmetry of the $^3C_{70}$ state has not been unambiguously determined up to now; the discussed options are D_{5h} and D_{2h}. Recent quantum chemical calculation of the D value reproduced its sign while the calculated value differs from the experimental ones by more than 10% [13].

Time-resolved EPR and OD EPR, as compared with normal continuous-wave (CW) EPR, suffer of much lower sensitivity. Also, both these techniques operate only under the condition of nonequilibrium spin polarization. The latter introduces additional parameters in the spectra simulation. So, CW EPR under thermal equilibrium seems to be a more precise approach to obtain exact values of D and E.

CW EPR spectra obtained under continuous light illumination (light-induced EPR) of photoexcited $^3C_{70}$ in methylcyclohexane were presented in early work [16], for the temperature range of 100–145 K where thermal equilibrium is achieved. However, the EPR line shape was discussed only qualitatively in this work. The purpose of the present work is to study in detail the $^3C_{70}$ EPR line shape in thermal equilibrium in different molecular glassy matrices as well as precise numerical

Table 1 $^3C_{70}$ ZFS parameters available in literature

T (K)	$\|D\|$ (G)	$\|E\|$ (G)	Solvent	Method	Ref.
5	55.7	7.4	Toluene	Time-resolved EPR	[4]
3, 77	52.5	7.5	Methylcyclohexane		[5, 6]
>77	56.7	7.4	Toluene		[7]
4.2	53.1	5.9	Polymethylmethacrylate (PMMA), methylcyclohexane		[8]
5–40	62	7	Toluene-polystyrene	Optically detected magnetic resonance	[9]
77	52	14	Toluene		[10]
4	58.9		Polystyrene		[11]
1.2	53.6	7.7	*n*-Pentane[a]		[12]
	53.9	10.7			
	42.9			Quantum chemical calculation	[13]

[a] ZFS parameters of two distinct sites in polycrystalline *n*-pentane matrix

simulations. ZFS parameters of $^3C_{70}$ found in this work turned out to be distributed within a noticeable range; such distribution seems to be a general property of the glassy state.

2 Experiment

Fullerene C_{70} (Aldrich, 99% purity) was dissolved at a concentration near 3×10^{-4} M in different organic solvents: decalin (1:1 mixture of *cis*- and *trans*-decalin, Sigma-Aldrich), *o*-terphenyl (Tokyo, "Kasei"), toluene (Moscow, "Mosreachim", distilled before using), and deuterated toluene-d_8 (St. Petersburg, "Izotop").

For the sample preparation of C_{70} embedded in polymethylmethacrylate (PMMA) (Aldrich, average molecular weight $\sim$ 996,000), both substances were soluted initially in toluene. Then the solvent was evaporated at a pressure of $\sim 10^{-2}$ Torr, and C_{70}/PMMA was deposited on a glass substrate, forming a film of about 100 μm thick.

All samples were put in quartz tubes with an outer diameter of 4.6 mm, liquid samples were frozen in liquid nitrogen to obtain transparent glasses.

Measurements were carried out on an X-band ELEXSYS ESP-580E EPR spectrometer. We used an ELEXSYS super high sensitivity probehead cavity equipped with an ER 4131VT temperature setting device (for CW EPR) or Bruker ER 4118 X-MD-5 dielectric cavity inside an Oxford Instruments CF 935 cryostat. Temperature was adjusted by cold nitrogen or helium gas flows and controlled by temperature controllers ER 4131VT or CF 935, which were calibrated with a copper–constantan thermocouple attached to the sample.

In CW EPR studies, microwave power was set to a value less than 0.63 mW that was low enough to avoid saturation effects. The magnetic field modulation frequency was 100 kHz, and its amplitude was set to 1 G. For *g*-factor measurements, a neutron-irradiated LiF sample was used [17] ($g = 2.00229 \pm 0.00001$).

In pulse EPR experiments, an electron spin echo signal was obtained as a function of magnetic field that is a so-called echo-detected (ED) EPR spectrum. To obtain the echo signal, a two-pulse microwave pulse sequence $\pi/2$–τ–π–echo was used, where $\pi/2$ and π pulses were 100 and 200 ns long, respectively, and the τ delay was 300 ns.

For sample photoexcitation, we used continuous irradiation from a Xe lamp, with a filter transmitting light in the range between 350 and 700 nm. The estimated light power reaching the sample was about 10 mW.

To suppress slight dark EPR signals, the experimental CW EPR spectra were obtained by subtraction of the CW EPR spectra obtained under light illumination and in the dark. In the pulse EPR experiment, no dark signal was detected.

Simulations were performed using an EasySpin (version 3.1.5) [18] program of the Matlab 6.5 package.

3 Results

3.1 Experimental CW EPR Spectra

In Fig. 1, experimental CW EPR spectra of $^3C_{70}$ in decalin at different temperatures are presented. At 30 K, the spectrum shows an apparent emissive/absorptive (E/A) pattern. With temperature increase above 70 K, the spectrum becomes fully absorptive. Similar spectra were obtained in other matrices (data not shown).

Above 50 K at the center region, an additional strong narrow peak arises, which increases and broadens with temperature increase. We found that the EPR spectral line shape and the relative intensity of wide and narrow spectral components do not depend on the C_{70} concentration in solution, microwave power (below the value where the saturation takes place), and intensity of the irradiating light (data not given).

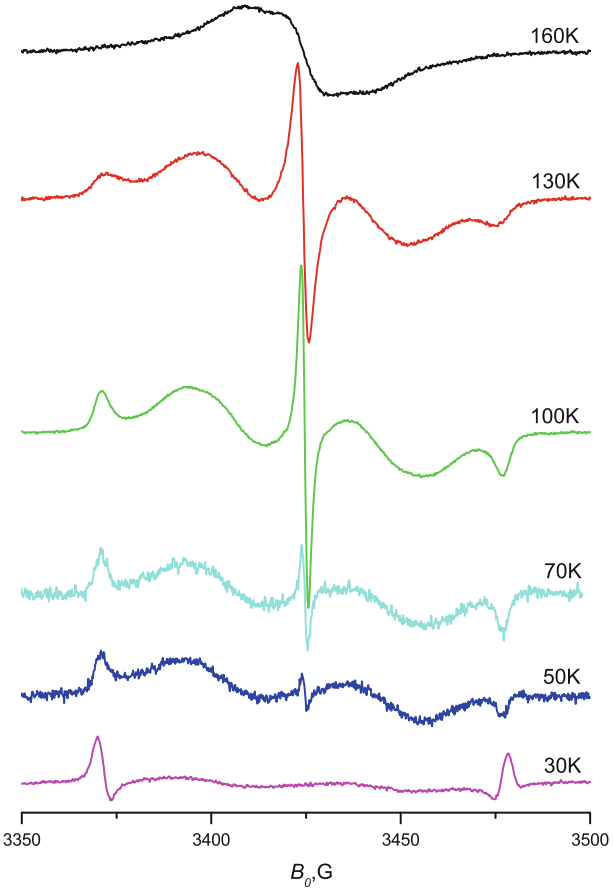

Fig. 1 CW EPR spectra of $^3C_{70}$ in decalin at 30–160 K. Microwave power is 63 μW (30–70 K) or 0.63 mW (100–160 K)

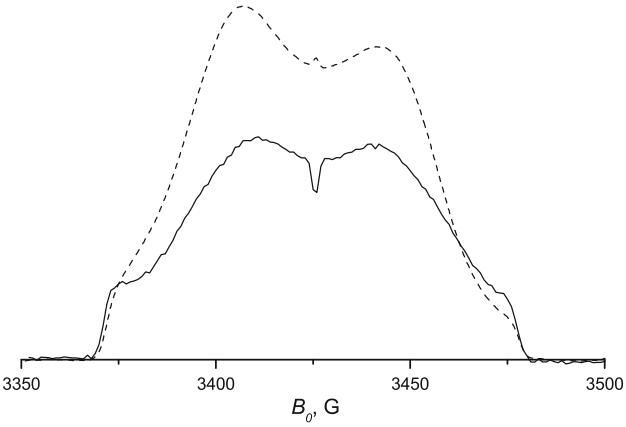

Fig. 2 ED EPR spectrum of $^3C_{70}$ in decalin at 50 K (*solid line*) compared with the CW EPR spectrum (*dashed line*) obtained at the same temperature (originally recorded as a first derivative (see Fig. 1) the spectrum was then digitally integrated). Spectra are artificially normalized to the same value of the low-field shoulders

In Fig. 2, ED EPR spectrum of $^3C_{70}$ in decalin at 50 K is shown (solid line). It is compared here with the CW EPR spectrum (dashed line in Fig. 2) taken at the same temperature (recorded originally as first derivative—see Fig. 1—it was then digitally integrated). Spectra of both types are artificially normalized to the same value of the low-field shoulder. One can see that after normalization the ED EPR intensity in the center of the spectrum is approximately twice smaller than the CW EPR intensity.

The CW EPR spectra of $^3C_{70}$ in toluene, toluene-d_8 decalin, *o*-terphenyl, and PMMA at temperature 77 K are shown in Figs. 3 and 4 (noisy lines).

With the replacement of normal toluene by deuterated toluene-d_8, the width of the narrow center peak is reduced from 1.2 to 0.65 G, which was measured from the CW EPR spectra obtained with 0.3 G modulation amplitude.

g-Factor of the narrow line peak was determined as 2.0025 ± 0.0001, for all matrices and temperatures studied. *g*-Factor of the broad line was determined using mean resonance magnetic fields for the low- and high-field spectrum extrema. It was found as 2.0029 ± 0.0003.

3.2 Numerical Simulation of CW EPR Spectra

Spin Hamiltonian of a triplet molecule consists of Zeeman and ZFS terms. Orientation of the magnetic field $\boldsymbol{B}_0$ direction in the triplet molecule framework is determined by polar and azimuthal angles θ and φ, respectively. In the laboratory framework, the Hamiltonian is

$$\boldsymbol{H} = g\beta \boldsymbol{B}_0 \boldsymbol{S} + \frac{1}{2}\left(\frac{D}{3}(3\cos^2\theta - 1) + E\sin^2\theta\cos 2\varphi\right)(3S_Z^2 - \boldsymbol{S}^2), \qquad (1)$$

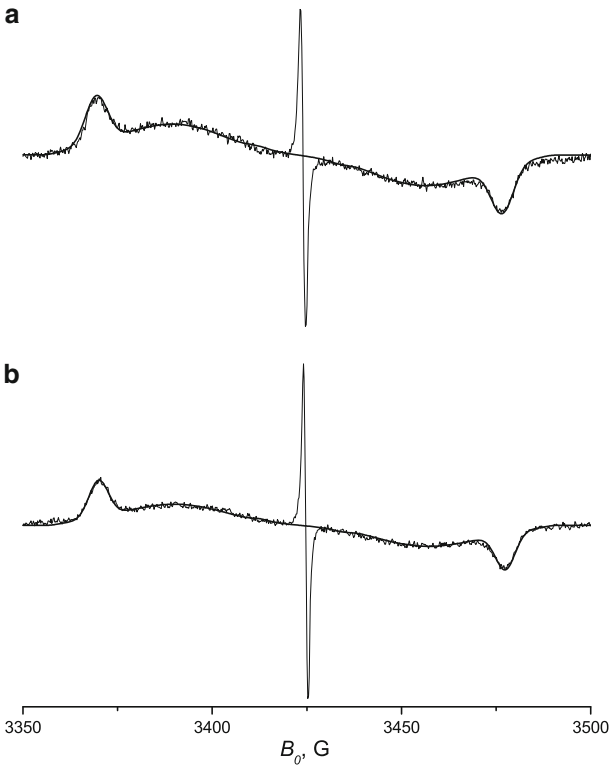

Fig. 3 Experimental CW EPR spectra (*noisy lines*) of C_{70} in normal toluene (**a**) and in toluene-d_8 (**b**) at 77 K. Microwave power is 63 mW. *Smooth lines* are simulations with the parameters given in Table 2

where $\boldsymbol{B}_0$ is the magnetic field, $\boldsymbol{S}$ and S_z are the spin operators ($S = 1$), β is the Bohr magneton, g is the g-factor, D and E are the ZFS parameters [19].

An EPR signal for each molecular orientation was calculated from Hamiltonian [Eq. (1)], using the matrix diagonalization method [18]. Then averaging of EPR signals of randomly oriented triplet molecules ensemble was performed. Boltzmann populations of the triplet sublevels were assumed. The D value was taken to be distributed by Gaussian probability, with a ΔD peak-to-peak width. The distribution of the E value was determined by the probability density function $W(E)$:

$$W(E) \sim E \exp\left(-\frac{E^2}{E_0^2}\right). \tag{2}$$

The other input parameters were the peak-to-peak width of the Gaussian individual line broadening, δ, and g-factor which was assumed to be isotropic, $g = 2.0029$.

The parameters of D and E distributions in simulations were varied independently. The derived best-fitted parameters are presented in Table 2. In Figs. 3 and 4, the results of simulations of experimental CW EPR spectra are shown (smooth lines). One can see quite a reasonable agreement between theory and experiment.

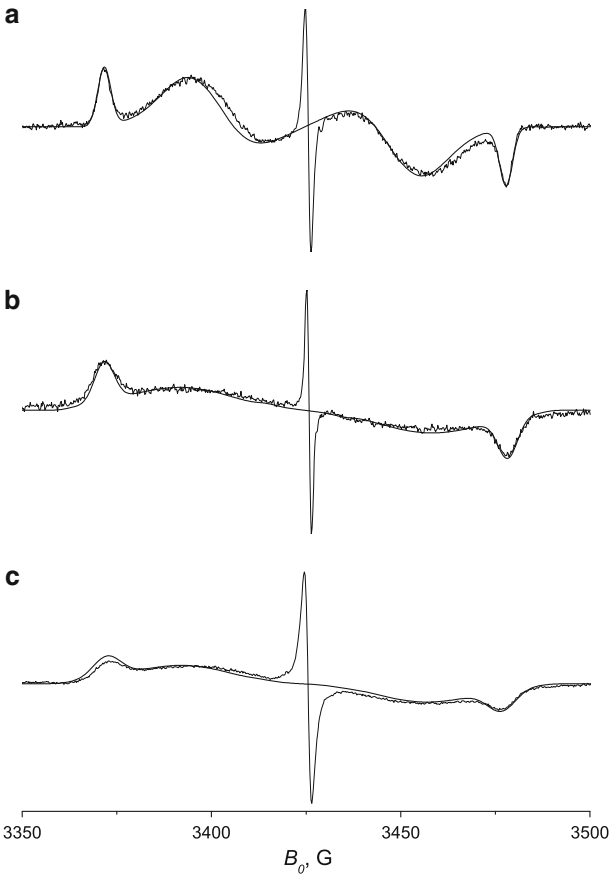

Fig. 4 Experimental CW EPR spectra (*noisy lines*) of $^3C_{70}$ in decalin (**a**), *o*-terphenyl (**b**), and PMMA (**c**) at 77 K. Microwave power is 63 μW. *Smooth lines* are simulations with parameters given in Table 2

Table 2 $^3C_{70}$ ZFS parameters obtained in this work at 77 K

Matrix	$\|D\|$ (G)	ΔD (G)[a]	E_0 (G)[b]	δ (G)[c]
Decalin	53.2 ± 0.2	1.6 ± 0.4	8 ± 2	3.0 ± 0.4
o-Terphenyl	53.5 ± 0.3	4.2 ± 0.8	15 ± 2	3.0 ± 0.8
PMMA	52.5 ± 0.5	7.8 ± 1.0	14 ± 2	3.0 ± 1.0
Toluene	54.0 ± 0.3	5.0 ± 0.8	15 ± 2	3.0 ± 0.8
Toluene-d_8				1.0 ± 0.8

[a] Peak-to-peak width of *D*-value Gaussian distribution

[b] Parameter of the density distribution function [Eq. (2)]

[c] Peak-to-peak line width of individual line Gaussian broadening

4 Discussion

The CW EPR line shapes of $^3C_{70}$ shown in Figs. 1, 3, and 4 are similar to those obtained previously (see, e.g., Ref. [16]). As one can see from Fig. 1, the $^3C_{70}$ EPR line shape changes dramatically with temperature variation. Below 50 K, it possesses an obvious E/A pattern, which may be readily explained by deviation of the triplet sublevels populations from the thermal equilibrium. A strong spin polarization of $^3C_{70}$ triplet sublevels immediately after photoexcitation was observed in time-resolved and pulse EPR experiments [5, 14, 20]. So, under our experimental conditions, at low temperatures the $^3C_{70}$ spin system does not relax to the Boltzmann equilibrium due to a long spin–lattice relaxation time. Above 70 K, the observed line shape acquires a purely absorptive pattern. Almost ideal antisymmetry of the first-derivative spectra testifies that the system is in thermal equilibrium and that anisotropy of g-tensor is negligible.

The EPR line shape changes seen in Fig. 1 above 130 K may be readily attributed to the glass transition of decalin (glass transition temperature $T_g = 137$ K). At 160 K, the edges of the spectrum are smeared out. This can be explained by molecular rotation of $^3C_{70}$, which partly averages the ZFS interaction.

With the replacement of normal toluene by deuterated toluene-d_8, the width of spectral edges of the broad peak decreased only slightly (Fig. 3). So, contribution of the unresolved hyperfine interaction with ambient magnetic nuclei should also be small. From the other hand, the width of the spectral edges is rather large (around 5 G). One possible reason for such a broadening could be the distribution of g-factor (g-strain). However, high-field pulse EPR study showed no significant g-strain for $^3C_{70}$ [21]. As the spectral edges correspond to canonical Z-orientation of $^3C_{70}$, we may suggest that this broadening is induced by distribution of D values (D-strain).

The important feature of spectra presented in Figs. 1, 2, 3 and 4 is the absence of peaks belonging to X and Y molecular axes, which are expected in the middle region of the spectra. The analogous result was obtained also in numerous previous studies [4–13]. The commonly accepted explanation of this effect is a possible influence of pseudorotation around the Z molecular axis, which would result in enhanced spin relaxation near the field positions corresponding to the X and Y molecular axes. To evaluate this acceleration, the ED EPR and CW EPR spectra are compared in Fig. 2. One can see that in the middle spectral region the ED EPR intensity is about twice smaller than the CW EPR one. This means that additional transversal relaxation here (which indeed may be caused by pseudorotation) occurs with a rate of $\sim 10^6$ rad/s. This value corresponds to a possible additional broadening of the CW EPR line shape of ~ 0.05 G.

Obviously, such broadening is too small to explain disappearance in the EPR spectra of the spectral features near canonical X and Y molecular orientations. Similarly, only very small anisotropy of transversal relaxation in $^3C_{70}$ was observed in the conditions of generating spin polarized $^3C_{70}$ by a laser pulse [20].

We may assume an alternative explanation of the effect of the absence of peaks belonging to X and Y molecular axes: the E value is also distributed within some range. To prove this suggestion, simulations of the spectral shape were performed with different types of the E probability density: a rectangle, a triangle, a Gaussian,

and the function given in Eq. (2). A good agreement between experimental CW EPR spectra in different glassy matrices was achieved only for the last function. The results of simulations are given in Figs. 3 and 4. Parameters of simulations are presented in Table 2.

Of course, the choice of *E*-distribution in the form of the function given by Eq. (2) is somewhat arbitrary. It is convenient because it depends only on one variable parameter. However, it presents the scale of possible variation of the *E* value.

The simulation parameters obtained are similar for all investigated matrices except for decalin, where ΔD and E_0 values are noticeably smaller. The *D* values do not depend significantly on the glassy matrix. They are close to those obtained previously in literature (see Table 1).

The distribution of the ZFS parameters may be caused by inhomogeneity of the local surrounding of $^3C_{70}$ molecules, which is naturally expected in a disordered glassy matrix. It is well established that $^3C_{70}$ experiences a Jahn–Teller distortion effect, and a non-zero *E* value appears because of reduction of the original D_{5d} ground state symmetry of the C_{70} molecule.

A rather large width of *E* distribution found here (see Table 2) indicates that the glassy matrix strongly influences the extent of this distortion. The mechanism behind this influence may be the change of vibronic energy surface of the $^3C_{70}$ molecule under the action of surrounding matrix molecules. Note that the $E = 0$ value cannot contribute to any possible *E*-distribution (otherwise the *X* and *Y* peaks would manifest themselves in experimental spectra), so the symmetry of most of $^3C_{70}$ molecules are reduced at least to the D_{2h} type. The presence of *E*-strain in triplet C_{70} was recently obtained in [22], where rectangular distribution of *E* values was suggested. Taking into account better quality of EPR spectra simulation in the present paper, we conclude that probability function $W(E)$ in Eq. (2) is more realistic.

The narrow peak in the center of the spectrum is puzzling. In early work [16], it was ascribed to fast isotropic rotation of some fraction of $^3C_{70}$ molecules, which averages out the ZFS tensor. This explanation, however, requires very fast isotropic molecular rotation (not pseudorotation around the *Z*-axis) of the $^3C_{70}$ molecule, with rotation correlation time $\tau_c \approx 10^{-11}$ s. (This value is determined from the relation $1/T_{2p} \approx \gamma^2 D^2 \tau_c$, with $T_{2p} \approx 100$ ns estimated from the width of this line at 77 K.) The possibility of such fast rotation for a large fullerene molecule in rigid glassy matrices at low temperature is under question.

The alternative explanation may be based on the coincidence of *g*-factors of the narrow peak and the *g*-factor for fullerene anion radical C_{70}^- [23, 24], which allows suggesting that the narrow line originates from C_{70}^- generated under light illumination. However, the presence of an electron donor in the vicinity of C_{70} is necessary for the C_{70}^- formation. One possibility is that some fraction of C_{70} molecules forms covalently linked dimers or higher order aggregates. The formation of such aggregates for C_{60} fullerenes was suggested in Ref. [25]. If it is the case also for C_{70}, light irradiation may result in intramolecular electron transfer in such dimers, with the formation of C_{70}^- and C_{70}^+. In the framework of this hypothesis, the increase of the narrow peak intensity with temperature increase may be

explained by thermal activation of the electron transfer, and its broadening may be explained by spin–spin relaxation time decrease due to fluctuation of magnetic interactions between C_{70}^- and C_{70}^+ at higher temperatures.

However, unambiguous assignment of the narrow line in the $^3C_{70}$ EPR spectrum demands further investigation.

5 Conclusion

The CW EPR spectra of C_{70} in decalin, *o*-terphenyl, PMMA, toluene and deuterated toluene were obtained under continuous visible light illumination in the temperature range of 30–160 K. At 30 K, spectra show an apparent emissive/absorptive (E/A) pattern. With temperature increase above 70 K, the spectra become fully absorptive. Deuteration of the solvent does not change significantly the $^3C_{70}$ EPR line shape and causes only a minor line narrowing.

Comparison of the CW EPR and ED EPR data allows estimating the influence of pseudorotation on the CW EPR line shape, this influence has turned out to be not decisive.

At 77 K, the triplet EPR spectra were simulated fairly well using the distribution of parameters *D* and *E*. This distribution (*D*- and *E*-strain) may be caused by inhomogeneity of local surrounding of $^3C_{70}$ in glassy matrices, which interplays with the $^3C_{70}$ Jahn–Teller distortions.

In addition to the broad triplet line, a narrow line in the center of the CW EPR spectrum was observed, its nature is briefly discussed. Probably, it can be attributed to fullerene anion radical C_{70}^-.

Acknowledgments This work was supported by the program of the Presidium of the Russian Academy of Sciences, project no. 27.55. We are grateful to Dr. F.G. Cherkasov (Zavoisky Physical-Technical Institute) for his gift of the LiF *g*-factor standard sample.

References

1. C.J. Brabec, S. Gowrisanker, J.J.M. Halls, D. Laird, S.J. Jia, S.P. Williams, Adv. Mater. **22**, 3839 (2010)
2. Z. Markovic, V. Trajkovic, Biomaterials **29**, 3561 (2008)
3. C.S. Foote, Top. Curr. Chem. **169**, 347 (1994)
4. M.R. Wasilewski, M.P. O'Neil, K.R. Lykke, M.J. Pellin, D.M. Gruen, J. Am. Chem. Soc. **113**, 2774 (1991)
5. M. Terazima, K. Sakurada, N. Hirota, H. Shinohara, Y. Saito, J. Phys. Chem. **97**, 5447 (1993)
6. M. Terazima, N. Hirota, H. Shinohara, Y. Saito, Chem. Phys. Lett. **195**, 333 (1992)
7. H. Levanon, V. Meiklyar, S. Michaeli, D. Gamliel, J. Am. Chem. Soc. **115**, 8722 (1993)
8. G. Agostini, C. Corvaja, L. Pasimeni, Chem. Phys. **202**, 349 (1996)
9. P.A. Lane, J. Shinar, Phys. Rev. B **51**, 10028 (1995)
10. C. Saal, N. Weiden, K.-P. Dinse, Appl. Magn. Reson. **11**, 335 (1996)
11. X. Wei, S. Jeglinski, O. Paredes, Z.V. Vardeny, Solid State Commun. **85**, 455 (1993)
12. M.V. Bronsveld, X.L.R. Dauw, E.J.J. Groenen, Chem. Phys. Lett. **293**, 528 (1998)
13. M. Gastel, J. Phys. Chem. A **114**, 10864 (2010)
14. X.L.R. Dauw, J. Visser, E.J.J. Groenen, J. Phys. Chem. A **106**, 3754 (2002)
15. M. Kallay, K. Nemeth, P.R. Surjan, J. Phys. Chem. A **102**, 1261 (1998)

16. G.L. Closs, P. Gautam, D. Zhang, P.J. Krusi, S.A. Hill, E. Wasserman, J. Phys. Chem. **96**, 5228 (1992)
17. F.G. Cherkasov, I.V. Ovchinnikov, A.N. Turanov, S.G. Lvov, V.A. Goncharov, A.Y. Vitols, Low Temp. Phys. **23**, 174 (1997)
18. S. Stoll, A. Schweiger, J. Magn. Reson. **178**, 42 (2006)
19. M.N. Uvarov, L.V. Kulik, M.A. Bizin, V.N. Ivanova, R.B. Zaripov, S.A. Dzuba, J. Phys. Chem. A **112**, 2519 (2008)
20. M.N. Uvarov, L.V. Kulik, S.A. Dzuba, J. Chem. Phys. **131**, 144501 (2009)
21. X.L.R. Dauw, O.G. Poluektov, J.B.M. Warntjes, M.V. Bronsveld, E.J.J. Groenen, J. Phys. Chem. A **102**, 3078 (1998)
22. M.N. Uvarov, L.V. Kulik, T.I. Pichugina, S.A. Dzuba, Spectrochim. Acta A **78**, 1548 (2011)
23. M. Baumgarten, L. Gherghel, Appl. Magn. Reson. **11**, 171 (1996)
24. J. Friedrich, P. Schweitzer, K.-P. Dinse, P. Rapta, A. Stasko, Appl. Magn. Reson. **7**, 415 (1994)
25. M. Bennati, A. Grupp, M. Mehring, J. Chem. Phys. **102**, 9457 (1995)